inorganics

MDPI

Article

Broadening the Scope of Polyoxometalates as Artificial Proteases in Surfactant Solutions: Hydrolysis of Ovalbumin by Zr(IV)-Substituted Keggin Complex

Nada D. Savić, David E. Salazar Marcano, Thomas Quanten and Tatjana N. Parac-Vogt *

Department of Chemistry, KU Leuven, Celestijnenlaan 200F, Box 2404, 3001 Leuven, Belgium; nada.savic@kuleuven.be (N.D.S.); david.salazarmarcano@kuleuven.be (D.E.S.M.); thomas.quanten@gmail.com (T.Q.)

* Correspondence: tatjana.vogt@kuleuven.be; Tel.: +32-16-32-76-12

Abstract: Development of catalysts for the selective hydrolysis of proteins is challenging, yet important for many applications in biotechnology and proteomics. The hydrolysis of hydrophobic proteins is particularly challenging, as due to their poor solubility, the use of surfactants is often required. In this study, the proteolytic potential of catalyst systems based on the Zr(IV)-substituted Keggin polyoxometalate $(Et_2NH_2)_{10}[Zr(PW_{11}O_{39})_2]$ (Zr-K 1:2) and three different surfactants (ionic SDS (sodium dodecyl sulfate); zwitterionic Zw3-12 (*n*-dodecyl-*N*,*N*-dimethyl-3-ammonio-1-propanesulfonate); and CHAPS (3-[(3-cholamidopropyl)dimethylammonio]-1-propanesulfonate)), which differ in structure and polarity, has been investigated. Hydrolysis of ovalbumin (OVA) was examined in the presence of Zr-K 1:2 and surfactants by sodium dodecyl sulfate poly(acrylamide) gel electrophoresis (SDS-PAGE), which showed the appearance of new polypeptide fragments at lower molecular weight, indicating that selective hydrolysis of OVA took place for all three catalyst systems. The same fragmentation pattern was observed, showing that the selectivity was not affected by surfactants. However, the surfactants influenced the performance of the catalyst. Hence, the interactions of OVA with surfactants and Zr-K 1:2 were investigated using different techniques such as tryptophan fluorescence, Circular Dichroism, and Dynamic Light Scattering. The speciation of the catalyst in surfactant solutions was also followed by ^{31}P Nuclear Magnetic Resonance spectroscopy providing insight into its stability under reaction conditions.

Keywords: polyoxometalate; zirconium; metalloproteases; ovalbumin; hydrolysis; surfactants

Citation: Savić, N.D.; Salazar Marcano, D.E.; Quanten, T.; Parac-Vogt, T.N. Broadening the Scope of Polyoxometalates as Artificial Proteases in Surfactant Solutions: Hydrolysis of Ovalbumin by Zr(IV)-Substituted Keggin Complex. *Inorganics* **2021**, *9*, 22. https://doi.org/10.3390/inorganics9040022

Academic Editor: Vladimir Arion

Received: 25 February 2021
Accepted: 23 March 2021
Published: 26 March 2021

1. Introduction

Membrane proteins are some of the most important molecules in living organisms and have a wide range of biological roles [1]. They are involved in fundamental cellular functions like cellular signaling, nutrient uptake, communication, motility and adhesion, metabolism, and ion transport [2]. It has also been estimated that more than 40% of currently used pharmaceutical drugs interact with transmembrane protein receptors. Bearing in mind their fundamental properties and importance in medical research, the study of their structure and function is of crucial importance. However, membrane proteins represent less than 1% of the structures deposited in the Protein Data Bank. Some of the main problems that hamper their structural characterization are their hydrophobic nature, large size, structural complexity, and relative lack of stability.

In the last decade proteomics has emerged as a powerful large-scale study of proteins, their structure, and physiological role or functions [3]. In the field of proteomics, controlled fragmentation of proteins is an important step that provides shorter protein fragments, which can be further analyzed by mass spectrometric techniques. Typically, natural proteases are used for this purpose, however the hydrophobic nature of membrane proteins makes the use of natural enzymes challenging. As membrane proteins are insoluble in

water, the addition of surfactants is a strategy that is often used in order to solubilize them. However, surfactants can lead to denaturation of the proteases used to cleave peptide bonds, resulting in disruption of their enzymatic activity [4], and therefore the use of artificial metalloproteases that preserve their catalytic activity in surfactant solutions has received growing interest as an attractive alternative.

Recently, our group has developed different materials based on metal-oxo clusters, including polyoxometalates (POMs), which can act as artificial metalloproteases. These materials have shown promising ability to cleave peptide bonds in proteins that have a large variety of intrinsic properties, such as differing isoelectric point (pI), size, and surface charge [5–14]. POMs represent a large class of anionic metal–oxide nanoclusters, which are composed of transition metals in their highest oxidation state. They exhibit broad structural diversity, exceptional physical properties, and have shown promising applications in the fields of catalysis, medicine, and optics, among others [15–17]. Frequently investigated POMs as catalysts towards the hydrolysis of different peptide bonds in proteins are usually based on the Keggin, Wells–Dawson, and Lindqvist structure types with Zr(IV), Hf(IV), or Ce(IV) embedded in their structure to form metal-substituted POMs (MS-POMs).

The main driving forces for the hydrolytic reactions catalyzed by MS-POMs are the electrostatic interactions between the negatively charged POM frameworks and positively charged patches on the protein surface, and the ensuing activation of peptide bonds by the strongly Lewis acidic Zr(IV), Hf(IV), or Ce(IV) metal centers coordinated to the POM. The hydrolysis reaction typically proceeds under mild pH conditions and produces large peptide fragments (3–15 kDa) that are well suited for applications in middle-down proteomic studies [5–14]. Furthermore, MS-POMs have been shown to maintain their activity towards peptide bond hydrolysis in surfactant solutions [18–21]. Interestingly, these studies with model proteins have shown that the extent to which surfactants influence the reactivity and selectivity of protein hydrolysis is largely dependent on the type of protein. For example, the selectivity of $[Zr(\alpha_2\text{-}P_2W_{17}O_{61})_2]^{16-}$ towards human serum albumin (HSA), which has a molecular weight (Mw) of 66.5 kDa, was influenced by the presence of 0.5 wt% CHAPS (3-[(3-cholamidopropyl)dimethylammonio]-1-propanesulfonate), since only four peptide bonds were cleaved in a neat HSA solution, while seven peptide bonds were hydrolyzed in the presence of the surfactant. The difference in selectivity was attributed to partial unfolding of HSA in the presence of CHAPS [19]. On the other hand, the selectivity of $[Zr(\alpha\text{-}PW_{11}O_{39})_2]^{10-}$ towards the hydrolysis of cytochrome c (Cyt c, Mw = 12.58 kDa), which is a much smaller protein compared to HSA, was not influenced by the presence of surfactants, as the same cleavage pattern was observed in the absence and in the presence of investigated surfactants. Although the selectivity of Cyt c hydrolysis remained unchanged, the surfactants influenced the rate of reaction, which was attributed to the conformational effects that surfactants had on the tertiary structure of the protein [20].

Even though surfactants play a vital role in the study of membrane proteins, they can also be attractive for probing the structure of globular water-soluble proteins. Both proteins and surfactants have charged and hydrophobic parts, so the interactions between surfactants and proteins are intrinsically complex processes which involve different types of intermolecular forces [22]. Therefore, small and well-established proteins are often used as models to study interactions and complex formations between proteins and surfactants. Generally, surfactants can be divided in two different types: denaturing (ionic) and non-denaturing (non-ionic) surfactants. Anionic surfactants, such as SDS (sodium *n*-dodecylsulfonate), have the ability to unfold the protein structure, whereas non-ionic surfactants leave the tertiary structure of the protein intact. The fact that the surfactants influence the three-dimensional structure of proteins [23] can be applied in the development of artificial proteases, since the partially unfolded state of the protein can allow for better access of the catalyst to peptide bonds that are buried within the native protein folding.

Considering the known ability of surfactants to affect protein structure and the fact that the hydrolysis of proteins in surfactant solutions has been scarcely explored, in this work hydrolysis of hen egg white ovalbumin (OVA) by $(Et_2NH_2)_{10}[Zr(\alpha\text{-}PW_{11}O_{39})_2]$ (Zr-K

1:2) (Figure 1) was investigated in the absence and in the presence of surfactants that are also used in the study of membrane proteins.

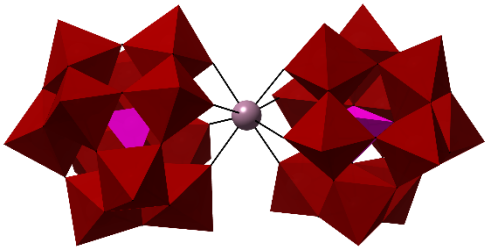

Figure 1. Polyhedral representation of $(Et_2NH_2)_{10}[Zr(\alpha\text{-}PW_{11}O_{39})_2]$ (Zr-K 1:2). WO_6 and PO_4 are represented by red octahedra and pink tetrahedra, respectively. The grey sphere represents Zr(IV) coordinated by Keggin units.

The surfactants used in this work, which are shown in Figure 2, differ in charge and polarity, and should therefore have different effects on the protein's three-dimensional structure. With an Mw of 44.3 kDa, in terms of size, OVA lies between the previously examined HSA and Cyt c, and therefore the current study is expected to provide more insight into the role of the protein structure and size in the hydrolysis by MS-POMs in surfactant solutions.

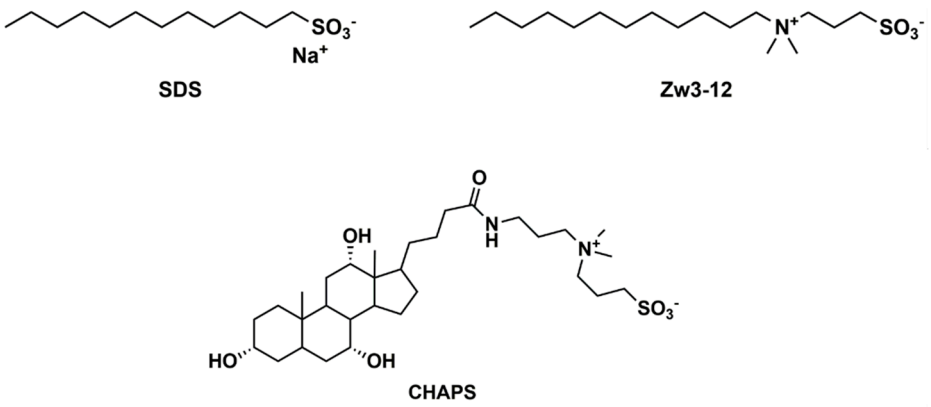

Figure 2. The chemical structures of the surfactants used in this study: SDS (sodium dodecyl sulfate); Zw3-12 (*n*-dodecyl-*N*,*N*-dimethyl-3-ammonio-1-propanesulfonate); and CHAPS (3-[(3-cholamidopropyl)dimethylammonio]-1-propanesulfonate).

2. Results and Discussion

2.1. Hydrolysis of OVA by Zr-K 1:2 in the Absence or Presence of Surfactants

OVA is a monomeric storage glycoprotein and is one of the main constituents of egg white for most avian species. It is composed of 385 amino acids, and its isoelectric point (pI) ranges from 4.43 to 4.66, which indicates that ovalbumin has a net negative charge of approximately −13.4 at physiological pH [24–26]. Additionally, OVA has a globular shape with a radius of around 3 nm [27], and approximately one half of its amino acid residues are hydrophobic, while one third are acidic in nature, making it a good model protein for the study of the hydrolysis of insoluble proteins [28]. The protein has a well-defined tertiary structure composed of nine α-helices and three β-sheets. It also has several carbohydrate and phosphate groups in its structure and can therefore be considered as a phosphoglycoprotein [24].

In the hydrolytic experiments performed in this work, 40 μM of OVA was incubated with 2 mM of Zr-K 1:2 at 60 °C in the absence and presence of different surfactants in order to explore the effect of surfactants on the efficiency and selectivity of protein hydrolysis. All samples were buffered at pH 7.4 by a 10 mM sodium phosphate buffer, and aliquots

were taken at different time intervals to monitor the progress of the hydrolytic reaction. The SDS-PAGE gel in Figure 3 shows the fragmentation pattern observed after 4 days of incubation at 60 °C.

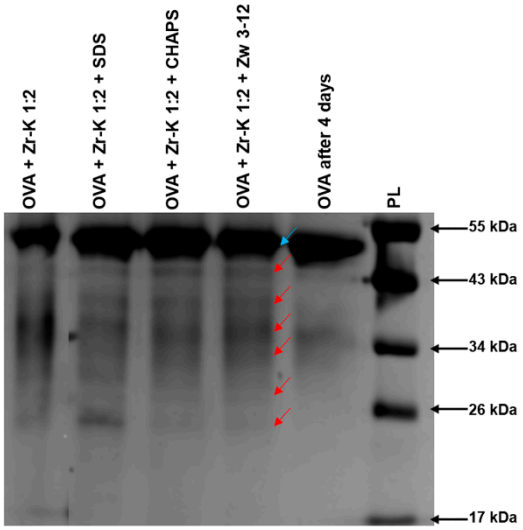

Figure 3. Silver-stained SDS-PAGE gel for the hydrolysis of 40 μM of OVA by 2 mM of Zr-K 1:2 at 60 °C after 4 days at pH 7.4 (10 mM sodium phosphate buffer) in the absence and presence of different surfactants. The values on the right side of the gel indicate the Mw reference in kDa. The blue (top) and red arrows indicate the intact protein and the hydrolytic fragments, respectively. The content of each lane is shown on top of the gel, and the concentration of each surfactant was 0.5 wt%. PL stands for protein ladder.

The appearance of six new fragments at lower Mw of approximately 42, 39, 36, 32, 26, and 24 kDa indicates that Zr-K 1:2 is able to hydrolyze OVA in solutions with and without surfactants. Interestingly, previously reported hydrolysis of OVA by a different MS-POM based on Hf(IV) and the Wells–Dawson POM structure, $K_{16}[Hf(\alpha_2\text{-}P_2W_{17}O_{61})_2]\cdot 19H_2O$ (Hf-WD 1:2), produced eight cleavage sites, which shows that the nature of Lewis acidic metal center and the POM scaffold has an influence on the selectivity of the hydrolysis [9].

Using ExPasy (the Expert Protein Analysis System) to predict the cleaved peptide bonds in the OVA primary sequence suggested that the five cleavage sites occurred at Asp-X bonds, which is in agreement with the previously established selectivity of POMs towards cleaving peptide bonds next to Asp residues [29]. In the presence of 0.5 wt% of all investigated surfactants, which is above their CMC (critical micellar concentration), the same fragmentation patterns were observed, indicating that the surfactants did not influence the selectivity of OVA hydrolysis by Zr-K 1:2. However, hydrolysis efficiency was different, and the obtained results suggest that the structure and nature of surfactants play a significant role in the hydrolytic reactions. While 57% of protein was cleaved in the absence of surfactants, only 20% was hydrolyzed in the presence of the anionic surfactant SDS. In the presence of zwitterionic surfactants Zw3-12 and CHAPS, approximately 35% of the protein was fragmented (Table 1).

Table 1. The hydrolysis efficiency of OVA hydrolysis by Zr-K 1:2 in the absence or presence of surfactants after 4 days of incubation at 60 °C and pH 7.4 (10 mM sodium phosphate buffer).

Surfactant	Hydrolysis Efficiency (%)
No surfactant	57
0.5 wt% (17.33 mM) SDS	20
0.5 wt% (8.13 mM) CHAPS	35
0.5 wt% (14.90 mM) Zw3-12	35

Several control experiments were also conducted under the same experimental conditions (60 °C in phosphate buffer (pH = 7.4, 10 mM)) in order to prove that Zr-K 1:2 is essential for the hydrolytic reaction to occur (Figure S1). In the presence of only surfactants, or upon addition of the monolacunary Keggin POM, which lacks the Zr(IV) metal center, no clear intense additional bands could be seen on the SDS-PAGE gel. Furthermore, in the presence of $ZrOCl_4 \cdot 8H_2O$, which was used for the synthesis of Zr-K 1:2, the formation of insoluble gels was observed, resulting in loss of the catalyst, in accordance with previously reported studies [5,6,30]. All these experiments unambiguously confirm that the presence of Zr-K 1:2, in which the POM scaffold stabilizes the Zr(IV) metal center, is essential for the hydrolytic reaction. Overall, the SDS-PAGE results suggest that the efficiency of OVA hydrolysis by Zr-K 1:2 largely depends on the nature of surfactants. Hence, in order to elucidate the observed effect of different surfactants on the hydrolysis of OVA, different spectroscopic techniques were employed.

2.2. Interaction between OVA and Zr-K 1:2 in the Absence or Presence of Surfactants

Tryptophan (Trp) fluorescence spectroscopy is one of the most convenient, sensitive, and non-destructive methods that is frequently used to study protein interactions [31,32]. Based on the intrinsic fluorescence of Trp amino acids present in a protein, which is very sensitive to the local environment, quantitative and qualitative information can be obtained about the interactions of compounds with proteins. OVA has 3 Trp residues in its primary sequence, two of which are solvent accessible, while the third is buried within the structure (Figure S2). As a result, since the fluorescence intensity and the wavelength at maximum intensity (λ_{max}) are strongly influenced by the environment of the Trp residues, Trp fluorescence is a suitable technique for investigating interactions between proteins and POMs [19,33–36].

The emission spectrum of OVA is characterized by a λ_{max} at 337 nm. Adding SDS or CHAPS to a 10 μM OVA solution resulted in a decrease in fluorescence intensity, without affecting the λ_{max} (Figure 4). A decrease of fluorescence intensity is indicative of protein unfolding, which is usually accompanied by a strong red shift of λ_{max} due to the exposure of the residue to the bulk solvent [37,38]. However, the lack of any red shift in this case suggests that the Trp buried within the structure is still found in a hydrophobic environment, suggesting that OVA is only partially unfolded or, alternatively, that the hydrophobic interior of the micelles formed by the surfactants might shield the Trp residues from solvent exposure.

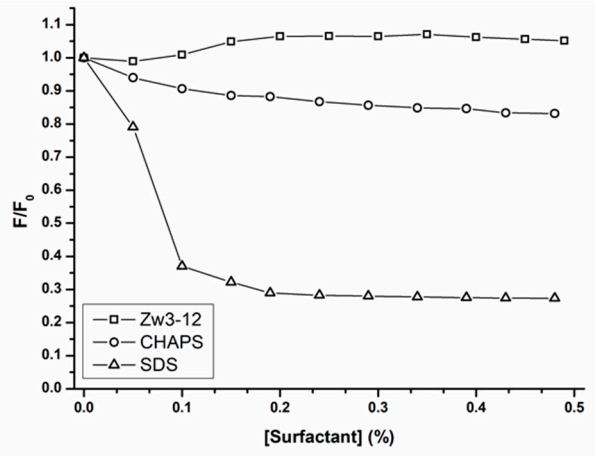

Figure 4. The emission intensity of 10 μM OVA at pH 7.4 (10 mM sodium phosphate buffer) in the presence of increasing concentrations of Zw3-12, CHAPS, or SDS. The λ_{max} is situated around 337 nm, and remained unaffected by the presence of surfactants.

The nature of the surfactant affects the degree to which OVA is unfolded. Harsh surfactants such as the anionic SDS caused the largest quenching of the fluorescence,

decreasing the intensity by 73% at a concentration of 0.1 wt%, while the zwitterionic surfactant CHAPS reduced the intensity by only 10% when added in the same amount. Zw3-12, on the other hand, caused only a negligible increase of fluorescence, suggesting that it had no significant influence on the environment around the tryptophan residues of OVA (Figure 4).

Adding Zr-K 1:2 stepwise (from 0 to 10 µM) to 10 µM OVA (in the absence or in the presence of surfactants) resulted in a gradual quenching of the fluorescence emission of OVA (Figure 5) due to interactions of the POM with the protein. The inset in Figure 5 shows the Stern–Volmer plot of the Trp fluorescence quenching of OVA by Zr-K 1:2. The linear relationship between F_0/F and [Zr-K 1:2] indicates that a static quenching mechanism applies, in which OVA and Zr-K 1:2 form a non-fluorescent complex [39]. Because of the linear Stern–Volmer plot, the quenching can be fitted to the derived Stern-Volmer equation:

$$log\left(\frac{F_0 - F}{F}\right) = log(K_a) + n \times log([Q]) \quad (1)$$

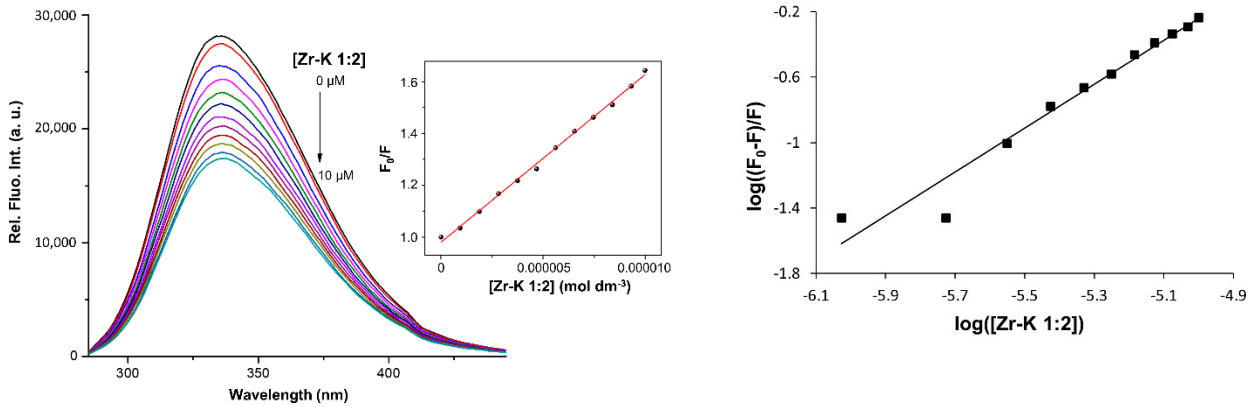

Figure 5. Emission spectra (**left**) of 10 µM OVA (in 10 mM sodium phosphate buffer at pH 7.4) in the absence or presence of different concentrations of Zr-K 1:2, which was increased from 0 µM (top spectrum) to 10 µM (bottom spectrum). The inset shows the Stern–Volmer plot where the ratio of unquenched (F_0) to the quenched fluorescence intensity (F) was plotted as a function of the concentration of Zr-K 1:2 ([Zr-K 1:2]). Derived Stern–Volmer plot (**right**) of $\log((F_0-F)/F)$ vs. log([Zr-K 1:2]) used to calculate the association constant (K_a) and the number of binding molecules (n).

In this equation, F_0 is the unquenched fluorescence intensity in the absence of the quencher, F the intensity in the presence of the quencher, K_a the association constant, n the number of bound quenching molecules, and [Q] the concentration of the quencher.

Equation (1) allows us to estimate the binding affinity (K_a) between the POM and OVA. Additionally, the stoichiometry of the POM/protein complex (n) can be determined. The calculated binding constants and complex stoichiometry in the absence or presence of surfactants are summarized in Table 2.

Table 2. The calculated binding constant (K_a) and stoichiometry (n) of the protein complexes formed between Zr-K 1:2 and OVA.

Surfactants	*n*	K_a (M^{-1})	R^2	Hydrolysis (%) after 4 Days
/	1.34	$2.86 \cdot 10^6$	0.9543	57
SDS	0.73	$2.47 \cdot 10^3$	0.9858	20
Zw3-12	0.97	$4.37 \cdot 10^4$	0.9953	35
CHAPS	0.84	$9.72 \cdot 10^3$	0.9724	35

Interestingly, the affinity constant of Zr-K 1:2 towards OVA is an order of magnitude higher in comparison to the binding constant of Hf-WD 1:2 [9]. This might be due to the

larger size and charge of Hf-substituted POM, since it is possible that Zr-K 1:2 being smaller makes it easier for it to approach the Trp residues on the protein surface in comparison with the larger and more rigid Hf-WD 1:2 species. This result is not surprising considering the net negative charge of the protein surface at physiological pH (−13.4) and the high net negative charge of Hf-WD 1:2 (−16), in contrast with the lower charge of Zr-K 1:2 (−10).

In the presence of 0.5 wt% SDS (Figure S3), the affinity constant of Zr-K 1:2 towards OVA is 3 orders of magnitude lower compared to when there is no added surfactant. This is most likely due to the presence of negatively charged polar heads of SDS, which, after binding to the protein, can repel the negatively charged POM and this results in a lower amount of POM molecules that can approach the protein surface. This is also reflected in the fewer number of bound POMs on the protein surface (n = 0.73 with SDS vs. n = 1.34 without surfactant). In the presence of zwitterionic surfactants Zw3-12 and CHAPS (Figures S4 and S5), the affinity constants are also lower compared to when there is no added surfactant, but the lowering of the POM binding affinity is not as pronounced as with SDS. Due to the zwitterionic nature of the surfactants with a cationic ammonium group, the repulsion of the POM by the protein/surfactant system is not as substantial. Hence, the POM is able to interact more easily with the protein in the presence of zwitterionic surfactants than in the presence of SDS due to its anionic nature.

2.3. Effect of Zr-K 1:2 and Surfactants on the Secondary Structure of OVA

The effect of Zw3-12, SDS, and CHAPS on the structure of OVA was examined further by Circular Dichroism (CD) spectroscopy. Proteins are characterized by secondary structure elements such as α-helices and β-sheets. The ordered stacking of peptide bonds in these structures causes a chiral effect that can be studied by far UV CD spectroscopy. The far UV region of a CD spectrum reflects the conformation of the backbone of a protein, making it a very suitable technique to determine structural changes in a protein [40–43]. The far UV CD spectra of OVA in the absence and in the presence of 0.5 wt% surfactants are shown in Figure 6.

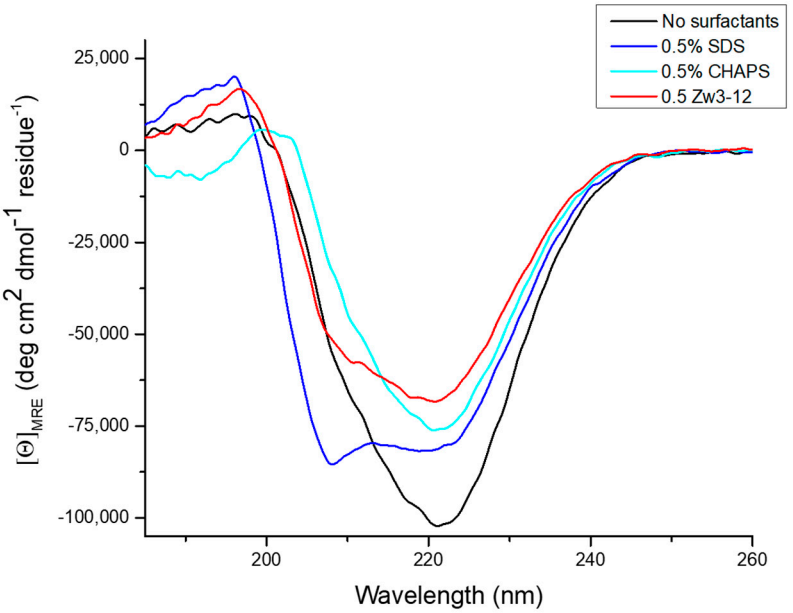

Figure 6. Mean residue ellipticity $[\theta]_{MRE}$ as a function of the wavelength of the far UV CD spectra of 10 μM OVA (black line) and 10 μM OVA in the presence of 0.5 wt% surfactants at 25 °C. All samples were buffered at pH 7.4 with a 10 mM sodium phosphate buffer.

The native structure of OVA is characterized by a major negative signal at 220 nm with a shoulder around 210 nm and an intense positive signal at 197 nm. The negative signal at 220 nm can be attributed to the presence of α-helical structure elements, while the smaller band at 210 nm is characteristic for proteins with significant quantities of β-sheet

structure [44]. This corresponds to the structural content of OVA, which has been previously reported to be approximately 45% β-sheets and 35% α-helices [45,46]. Interestingly, as can be seen from Figure 6, all three surfactants have a different influence on the secondary structure of the protein. Adding 0.5 wt% of Zw3-12 caused a small restructuring of OVA as the signal intensity of the negative peak at 220 nm decreased, while the positive signal at 197 nm increased, with the shoulder at 210 nm becoming more pronounced. Much larger restructuring was observed in the presence of 0.5 wt% SDS, where a strong negative signal emerged at 208 nm and the trough at 220 nm deepened. A blue shift was observed for both positive and negative CD peaks, which is in accordance with the previously published data of Zemser et al., where SDS had the same effect on the secondary structure of OVA [44]. In the presence of 0.5 wt% of CHAPS, the shape of the CD spectrum did not change significantly, but a slight decrease of the positive and negative signals was observed, which is comparable to the changes in peak intensity observed for the other zwitterionic surfactant, Zw3-12. Although both surfactants are zwitterionic in nature, CHAPS has a partially hydrophilic structure with a hydroxyl-functionalized steroid skeleton as a tail, while Zw3-12 has hydrophobic dodecyl chain, which makes it more prone to interact with hydrophobic parts of the protein. Since OVA consists of a large hydrophobic core [28], it is not surprising that its structure is more affected in the presence of Zw3-12 in comparison with CHAPS.

The effect of Zr-K 1:2 on the secondary structure of OVA was also studied in the absence and presence of different surfactants (Figure 7). Binding of the POM to OVA did not significantly affect the shape of the spectra, as the depression at 210 nm and the peak at 197 nm became less pronounced, and the trough at 220 nm stayed constant (Figure 7I). However, the addition of even a small amount of Zr-K 1:2 caused a significant decrease in the intensity of the negative CD signal, indicating that restructuring of the protein took place (Figure 7I). However, higher concentrations of Zr-K 1:2 were needed to cause visible changes in the CD spectra obtained for solutions of OVA with 0.5 wt% Zw3-12, CHAPS or SDS, which is consistent with the formation of a micellar/protein super structure [47] that hinders interactions between POM and protein.

Overall, the CD results are consistent with the findings from the Trp fluorescence studies, in which zwitterionic surfactants did not cause significant perturbation of the native protein structure (Figure 4). The CD spectra of OVA in solution with 0.5 wt% Zw3-12 or 0.5 wt% CHAPS in the absence of POM had a similar shape to the spectrum of OVA in the absence of surfactants, indicating that these surfactants did not significantly change the secondary structure of OVA (Figure 8). In contrast to the zwitterionic surfactants, the conformation of OVA in the presence of SDS underwent more significant changes, resulting in an increase in the α-helical content. This increase in the secondary structure of the protein might be the result of a more open tertiary structure, as has been previously observed [48,49]. Such an open tertiary structure is likely to cause hydrophobic patches of the protein to be more exposed towards interactions with the hydrophobic tails of surfactants, allowing dense micellar formation around unfolded OVA, thus preventing POM/protein interactions (Figure 8). In addition, previously reported data has shown that SDS interacts with OVA at very low concentrations mainly via hydrophobic interactions [47]. In addition, electrostatic interactions in which Na^+ counterions of SDS are absorbed onto the surface of the protein, resulting in the release of water molecules, have also been suggested [47]. In the latter case the hydrophobic alkyl chains of SDS are solvent exposed, which can potentially sterically hinder interactions of the POM with the protein (Figure 8). This is also consistent with the observation that in the presence of 0.5 wt% SDS, the addition of Zr-K 1:2 causes a more pronounced red shift in the CD spectra, suggesting that the secondary structure of OVA needs to undergo larger changes in order to accommodate the POM.

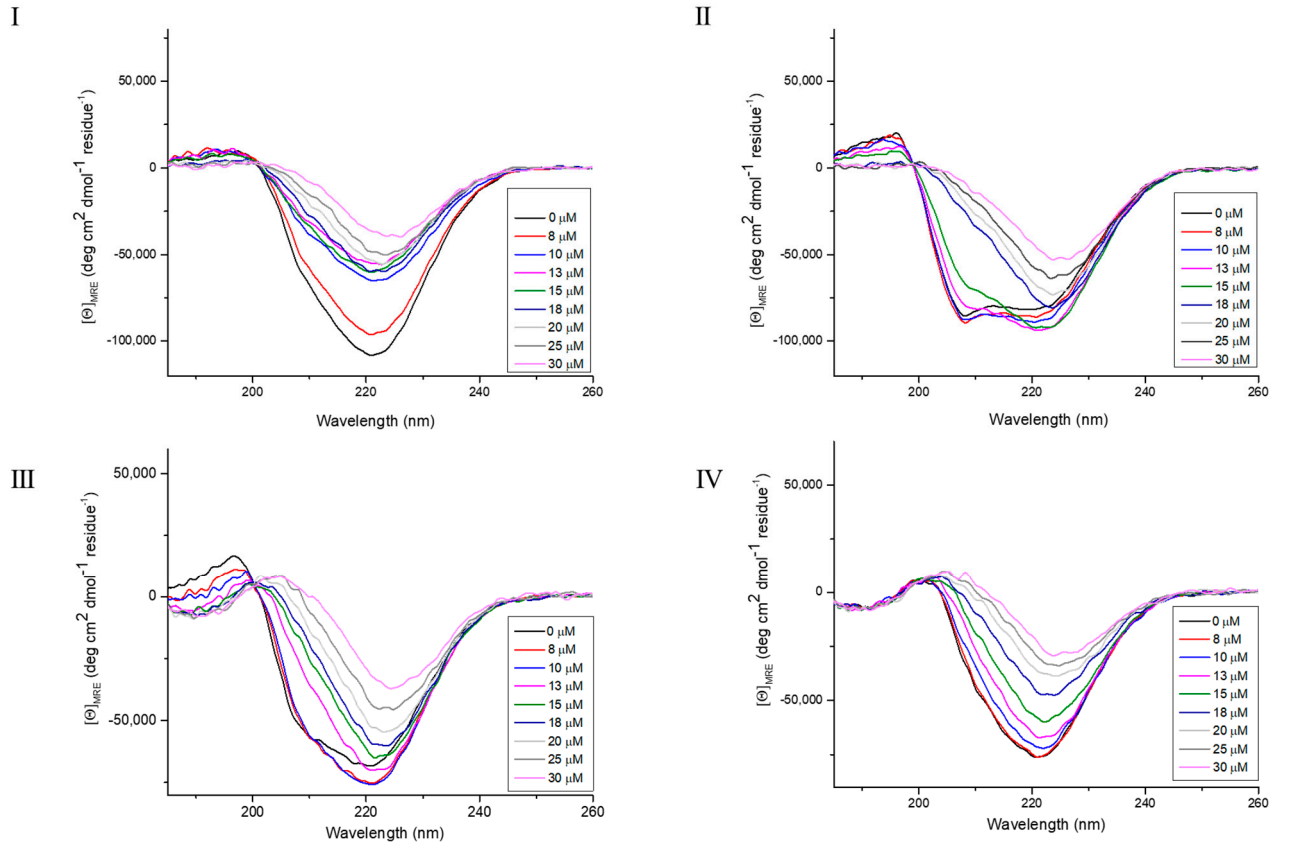

Figure 7. Far UV CD spectra of 10 μM OVA solutions in the presence of increasing concentrations of Zr-K 1:2 (from 0 to 30 μM) in the absence of surfactants, (**I**) as well as in the presence of 0.5 wt% SDS (**II**), 0.5 wt% Zw3-12 (**III**), and 0.5 wt% CHAPS (**IV**). All samples were buffered at pH 7.4 by a 10 mM sodium phosphate buffer and kept at 25 ± 0.1 °C during measurements.

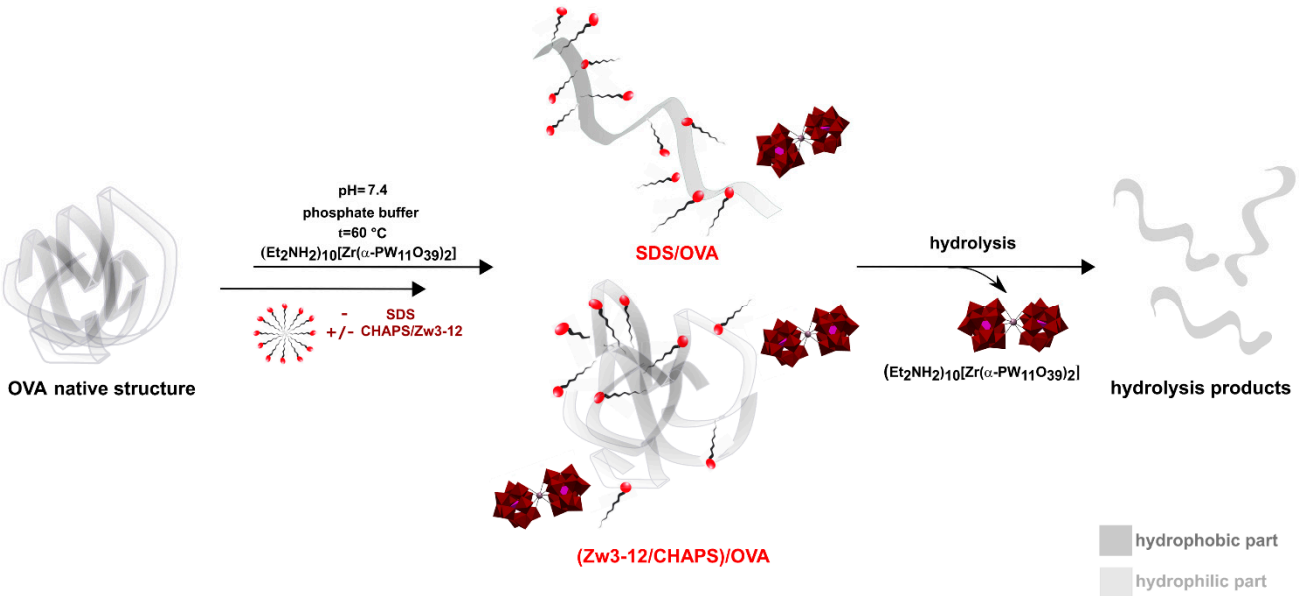

Figure 8. Schematic representation of the interaction between OVA and Zr(IV)-substituted Keggin-type POM, $(Et_2NH_2)_{10}[Zr(\alpha\text{-}PW_{11}O_{39})_2]$ (Zr-K 1:2) in the presence and absence of different surfactants.

2.4. Particle Size Distribution and Zeta Potential

The formation of micellar structures around the protein for solutions of 40 μM OVA in 10 mM phosphate buffer at pH 7.4 in the presence of surfactants, under similar conditions to those used for hydrolysis, were investigated by Dynamic Light Scattering (DLS) to determine the particle size distribution (PSD) of the solutions (Figure 9I). The influence of surfactants on the surface charge of the protein was also observed by measuring the zeta potential (ζ) via electrophoresis and laser Doppler velocimetry (Figure 9II). A solution of 40 μM OVA on its own in phosphate buffer gave rise to two peaks in the intensity PSD corresponding to particles with a hydrodynamic diameter (d_H) of 6.5 nm and 43.8 nm. The first peak at 6.5 nm corresponds to the expected d_H of OVA [27], while the peak at 43.8 nm is due to trace amounts of aggregates of OVA as previously reported by Visentini et al. [50]. ζ for OVA in this solution was −9.4 mV, as expected for a protein with a pI of 4.43 to 4.66 and in accordance with the literature [50]. In agreement with the Trp fluorescence and CD results, OVA in the presence of 0.5 wt% SDS produced larger particles with d_H of 8.7 nm and 79–190 nm due to the formation of micellar structures, which most likely results in unfolding of the protein. Due to the anionic nature of SDS, the surface charge of particles in solution also became significantly more negative as reflected by a ζ of −59.9 mV. The formation of large micellar structures with a significant negative surface charge likely prevents Zr-K 1:2 from approaching the protein, resulting in a significantly lower hydrolytic efficiency. In contrast, 0.5 wt% CHAPS in the protein solution had only a small effect on ζ and the intensity PSD: ζ became slightly more negative (−15.9 mV), and the particle size only increased slightly to give peaks with a d_H of 7.5 nm and 43.8 nm, corresponding to the formation of a micelle around the protein without significantly changing the structure of the protein or its aggregates as observed by CD spectroscopy, which showed only slight changes in the CD signal due to 0.5 wt% CHAPS while the shape of the CD spectrum remained the same. As with CHAPS, the presence of 0.5 wt% Zw3-12 also produced very few changes in ζ and the intensity PSD: ζ also became slightly more negative (−16.3 mV), but d_H for the aggregates seemed to decrease slightly to 32.7 nm, which is likely due to the more hydrophobic nature of Zw3-12 allowing for the formation of smaller aggregates in solution as Zw3-12 interacts more strongly with hydrophobic regions of the protein, matching what was observed by CD spectroscopy. The lower surface charge and smaller size of the micellar structures formed by the zwitterionic surfactants in comparison with SDS explains why the hydrolytic efficiency was higher for these surfactants. Each surfactant interacts in different ways with the protein due to differences in their hydrophobicity and ionic character (Figure 8).

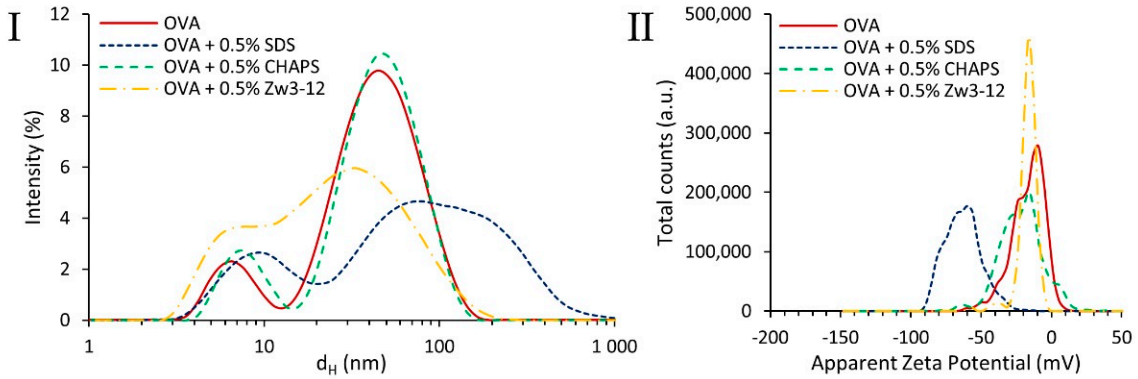

Figure 9. Intensity particle size distribution (PSD) of 40 μM OVA (solid red line) in the presence and absence of 0.5 wt% of surfactants (dashed lines) in 10 mM phosphate buffer at pH 7.4 (**I**), resulting in particles with different hydrodynamic diameter (d_H), and the apparent zeta potential (ζ) for the same solutions (**II**).

2.5. ^{31}P NMR Stability Study

^{31}P NMR spectroscopy was also used in order to gain further insight into the stability of Zr-K 1:2 in the presence and absence of surfactants and the protein. The measurements were performed on solutions containing Zr-K 1:2 (2 mM) in 10 mM phosphate buffer at pH 7.4, with and without the addition of OVA (20 μM) and/or 0.5 wt% surfactant. All solutions were incubated at 60 °C for up to 7 days, and ^{31}P NMR spectra were recorded at different time intervals (Figures S6–S12).

The ^{31}P NMR signals at −14.78 and −14.86 ppm correspond to Zr-K 1:2, and originate from different P–O bond lengths and angles in the two Keggin units of Zr-K 1:2 [31]. In all spectra, the appearance of a minor signal at −10.5 ppm indicates the presence of a lacunary Keggin POM, $[PW_{11}O_{39}]^{7-}$, which forms immediately after mixing. The lacunary Keggin POM most likely forms due to the presence of the phosphate buffer, which is able to sequester the Zr(IV) metal center from Zr-K 1:2, since in pure D_2O the lacunary Keggin POM was not observed [30]. In addition, it is well known that Zr-K 1:2 undergoes very fast equilibria in solution, resulting in the formation of the monomeric $[Zr(\alpha\text{-}PW_{11}O_{39})]^{3-}$ (Zr-K 1:1) POM, which is presumed to be the catalytically active species [51]. The presence of the monomeric Zr-K 1:1 is difficult to detect in solution, but its formation has been previously confirmed by single crystal X-ray diffraction, where it was observed in a non-covalent complex with hen egg white lysozyme [51].

In terms of the stability and speciation of the catalyst, no significant changes in ^{31}P NMR spectra of Zr-K 1:2 were observed during the incubation in the presence of all surfactants, regardless of the presence or absence of OVA. The obtained results also suggest that SDS does not have any observable interactions with Zr-K 1:2, nor does it influence its structure, which is not surprising as both POM and SDS are negatively charged (Figures S6–S8). However, the ^{31}P NMR spectra of Zr-K 1:2 recorded in the presence of CHAPS and Zw3-12 showed a large shift of ^{31}P resonance of Zr-K 1:2 from to −14.78 to 13.70 ppm, suggesting interactions between Zr-K 1:2 and zwitterionic surfactant. The same ^{31}P NMR spectra were observed when OVA was added to the solution, implying that protein does not significantly influence this interaction (Figures S9–S12). These results are in accordance with a previously published study, where zwitterionic surfactants (CHAPS and Zw3-12) were shown to interact with the negatively charged POM via the positively charged ammonium group, while not affecting the catalytic activity of the POM [18].

3. Materials and Methods

3.1. Materials

N,*N*,*N*′,*N*′-tetramethylethylenediamine (TEMED), ammonium persulphate (APS), phosphotungstic acid hydrate ($H_3[PW_{12}O_{40}]\cdot xH_2O$), sodium tungstate dihydrate ($Na_2WO_4\cdot 2H_2O$), glycine, disodium phosphate (Na_2HPO_4), sodium, dodecyl sulfate (SDS), *n*-dodecyl-*N*,*N*-dimethyl-3-ammonio-1-propanesulfonate (Zw3-12), 3-[(3-cholamidopropyl)dimethylammonio]-1-propanesulfonate (CHAPS), formaldehyde, glutaraldehyde, silver nitrate, sodium thiosulphate, glycerol, hen egg white ovalbumin (OVA) (≥98% purity), and bromophenol blue were purchased from Sigma-Aldrich (St. Louis, MO, USA). Zirconium oxychloride octahydrate and acetone were obtained from ChemLab (Zedelgem, Belgium). Aqueous hydrochloric acid (37%), sodium hydrogen carbonate, and sodium carbonate were obtained from Acros organics (Fair Lawn, NJ, USA). Ethanol, methanol, aqueous ortho-phosphoric acid (85%), glacial acetic acid, diethyalaminehydrochloride, and protein ladders were acquired from Thermo Fisher Scientific (Waltham, MA, USA). Monosodiumphosphate (NaH_2PO_4) was purchased from VWR Chemicals (Radnor, PA, USA). Tris(hydroxymethyl)aminomethane (TRIS), acrylamide:bisacrylamide (29:1) solution (40%), and acrylamide:bisacrylamide (19:1) solution (40%) were procured from AppliChem Panreac (Darmstadt, Germany). 2-mercaptoethanol was purchased from Merck (Darmstadt, Germany). $[Zr(\alpha\text{-}PW_{11}O_{39})_2]^{10-}$ was synthesized following a slightly altered procedure from [52].

3.2. Methods

3.2.1. Hydrolysis Experiments

Solutions containing 40 μM of OVA and 50 equivalents of Zr-K 1:2 in the presence or absence of the different surfactants (0.5 wt% CHAPS, SDS, or Zw3-12) were prepared in 10 mM sodium phosphate buffer at pH 7.4. The samples were incubated for several days at 60 °C in micro centrifuge tubes in a Thermomixer (Eppendorf, Hamburg, Germany) and aliquots were taken at several time intervals. SDS-PAGE was used to monitor the progress of the hydrolysis (4% stacking gels and 16% resolving gels in a Tris-Glycine and 0.1% SDS running buffer). For each sample, 10 μL was mixed with 5 μL of sample buffer (250 mM DTT, 50% glycerol, 5% SDS, 0.05% bromophenol blue, 225 mM Tris HCl buffer, pH 6.8) and incubated at 95 °C for 5 min. After 3 min of centrifugation, 10 μL of the final sample solution was loaded on a 16% gel. The PageRuler™ Prestained Protein Ladder was used as a Mw reference. The gels were run at 200 V and 35 mA/gel current, with the maximum power set to 50 W using an OmniPage electrophoretic cell combined with an EV243 power supply. Total running time was approximately 1.5 h. The gels were developed with silver staining and analyzed using a GelDoc EZ setup with the Image Lab software (Bio-Rad, Hercules, CA, USA).

3.2.2. Fluorescence Spectroscopy

Samples containing 10 μM OVA neat or in the presence of 0 to 0.5 wt% SDS, CHAPS, or Zw3-12 were prepared in a 10 mM sodium phosphate buffer at pH 7.4. For the 0.5 wt% surfactant solutions, the concentration of Zr-K 1:2 was increased from 0 to 10 μM to observe the interactions of the POM with the protein. The samples were kept at ambient temperature during the acquisition of the spectra. A 10.0 mm quartz cuvette was used to record emission spectra using an Edinburgh Instruments FLS-980 spectrometer (Edinburgh Instruments, Livingston, UK). The samples were excited at 280 nm, and emission was observed from 285 to 450 nm with a maximum at approximately 337 nm. Data were analyzed in Origin Pro 8.0 (Origin 2018b (academic), OriginLab, Northampton, MA, USA).

3.2.3. Circular Dichroism Spectroscopy

Solutions containing 10 μM OVA in the absence and presence of 0.5 wt% SDS, Zw3-12, and CHAPS were prepared in a 10 mM sodium phosphate buffer at pH 7.4. To observe the effect of the POM on the protein structure, the concentration of Zr-K 1:2 was increased incrementally from 0 to 30 μM. The samples were kept at a constant temperature of 25 ± 0.1 °C during the recording of all spectra. The CD spectra were recorded with a JASCO 1500 spectrometer (Jasco, Oklahoma City, OK, USA) directly after the samples were prepared, using a 1 mm quartz cuvette. The resulting spectra are averaged over 3 accumulations with a bandwidth of 1 nm. The phosphate buffer solution (10 mM, pH 7.4) was measured for baseline correction. The machine response (θ in mdeg) was converted to mean residue ellipticity ([θ]MRE) according to the following equation [53]:

$$[\theta]_{MRE} = \frac{\theta \times 0.1 \times \langle M \rangle}{c_g \times l_{cm}} = \frac{\theta}{c_M \times n \times l_{mm}} \quad (2)$$

where <*M*> is the mean residue molar weight (equal to $M_w/(n-1)$); c_g and c_M are the protein concentration in g/L and mol/L, respectively; l_{cm} and l_{mm} are the optical pathlength in cm and mm, respectively, and n is the number of peptide bonds in the protein (equal to the total number of amino acids minus one). Origin Pro 8.0 (Origin 2018b (academic), OriginLab, Northampton, MA, USA) was used for data analysis.

3.2.4. Particle Size Distribution and Zeta Potential

The particle size distribution (PSD) and zeta potential (ζ) of solutions of 40 μM OVA in 10 mM sodium phosphate buffer at pH 7.4 in the presence or absence of different surfactants (0.5 wt% CHAPS, SDS, or Zw3-12) at 25 °C were determined by measuring the

backscattering at 173° of a 632.8 nm laser using a Zetasizer Nano ZSP (Malvern Panalytical Ltd., Malvern, UK). Prior to measurement, all samples were prepared from a buffer solution filtered through a 0.2 μm nylon filter, and then the solutions were centrifuged at 14k rpm for 15 min to remove any large undesired particles due to dust or impurities. All measurements were performed using folded capillary cells. The hydrodynamic diameter (d_H) of particles in solution was determined from the average intensity PSD of 3 measurements of the intensity PSD as calculated from the Dynamic Light Scattering correlation data by the equipment software provided by the manufacturer (Zetasizer Software 7.12, Malvern Panalytical Ltd., Malvern, UK). The zeta potential of the particles in solution was determined by electrophoresis and laser Doppler velocimetry according to the Smoluchowski model [54], using the equipment's software.

3.2.5. ^{31}P NMR Spectroscopy

^{31}P NMR spectra were recorded on a Bruker Avance 400 (161.98 MHz) spectrometer (Bruker, Billerica, MA, USA). Solutions containing 2 mM of Zr-K 1:2, and 0.5 wt% of surfactants (SDS, Zw3-12, CHAPS) with and without 20 μM of OVA were prepared in 10 mM phosphate buffer at pH 7.4. ^{31}P NMR spectra of all samples were measured at different incubation times for up to 7 days. For each measurement, 500 μL of the sample was taken and 2 drops of D_2O were added. As an external standard, 25% H_3PO_4 in D_2O in a sealed capillary was used.

4. Conclusions

In this study, the reactivity and selectivity of the Zr(IV)-substituted Keggin polyoxometalate towards the hydrolysis of ovalbumin has been investigated in the presence of different surfactants typically used for protein solubilization. The selectivity of the POM towards hydrolysis of OVA was not affected by the presence of 0.5 wt% SDS, CHAPS, or Zw3-12 surfactants, suggesting that the previously observed affinity of POMs towards hydrolyzing peptide bonds next to Asp residues is largely independent of protein conformation. Although the presence of surfactants does not alter the selectivity of OVA hydrolysis, the efficiency of the reaction was affected differently depending on the type of surfactant. All 3 surfactants slowed down the protein hydrolysis reaction, but this effect was more pronounced for the anionic SDS than for the zwitterionic CHAPS and Zw3-12 surfactants. Trp fluorescence quenching results demonstrated that surfactants decrease binding affinity between POM and OVA, most likely due to the formation of protein/micellar complexes. Interestingly, although SDS caused the largest unfolding of the protein, the affinity of POM towards OVA in SDS solution was lowest, which is due to repulsion between like charges and the formation of a more opened conformation of the protein that facilitates dense micellar formation of SDS molecules around hydrophobic protein patches, thereby attenuating interactions between the protein and Zr-K 1:2. However, the zwitterionic surfactants have a less noticeable effect on the protein conformation, exposing less hydrophobic residues to the surface, and therefore formation of protein micellar system is less pronounced, which was additionally confirmed by DLS and CD spectroscopy. The results from this study suggest that surfactants can be used as additives in POM-promoted protein hydrolysis, but the efficiency of hydrolysis largely depends on the type of the surfactant used. Depending on the nature and the concentration of the surfactant, formation of different micellar complexes can occur which affect the effective interaction with the catalyst. Nevertheless, the POM catalyst retains its selectivity and activity, further showcasing the potential of POMs as artificial proteases that can be used for hydrolysis of hydrophobic or poorly soluble proteins.

Supplementary Materials: The following are available online at https://www.mdpi.com/article/10.3390/inorganics9040022/s1, Figures S1–S12: SDS-PAGE gels, Tryptophan fluorescence quenching spectra, Stern–Volmer plots, ^{31}P NMR spectra.

Author Contributions: All experimental work was performed by N.D.S., D.E.S.M., and T.Q. Data analysis was performed by N.D.S., D.E.S.M., and T.Q., with valuable contributions and corrections from T.N.P.-V. The manuscript was written by N.D.S., D.E.S.M., and T.Q., with valuable contributions and corrections from T.N.P.-V. All authors have read and agreed to the published version of the manuscript.

Funding: T.N.P.-V. thanks KU Leuven and Research Foundation Flanders (FWO) for funding under grant G0D3219N. T.N.P.-V. is also grateful to the European Commission for funding under the Horizon 2020, FoodEnTwin project, GA No. 810752.

Institutional Review Board Statement: Not applicable.

Informed Consent Statement: Not applicable.

Data Availability Statement: Data is contained within the article or supplementary material. Additional details about the data are also available on request from the corresponding author.

Acknowledgments: T.N.P.-V. thanks Science Foundation Flanders (FWO) and KU Leuven for funding. N.D.S. acknowledges KU Leuven for financial support, and D.E.S.M. acknowledges Science Foundation Flanders (FWO) for a PhD fellowship (83523/1183021N).

Conflicts of Interest: The authors declare that the research was conducted in the absence of any commercial or financial relationships that could be construed as a potential conflict of interest.

References

1. Scott, K.A.; Bond, P.J.; Ivetac, A.; Chetwynd, A.P.; Khalid, S.; Sansom, M.S.P. Coarse-Grained MD simulations of membrane protein-bilayer self-assembly. *Structure* **2008**, *16*, 621–630. [CrossRef]
2. Lee, S.C.; Knowles, T.J.; Postis, V.L.G.; Jamshad, M.; Parslow, R.A.; Lin, Y.-P.; Goldman, A.; Sridhar, P.; Overduin, M.; Muench, S.P.; et al. A method for detergent-free isolation of membrane proteins in their local lipid environment. *Nat. Protoc.* **2016**, *11*, 1149–1162. [CrossRef]
3. Shah, T.R.; Misra, A. *Challenges in Delivery of Therapeutic Genomics and Proteomics*; Elsevier: London, UK, 2011; pp. 387–427.
4. Guzman, M.L.; Marques, M.R.; Me, M.E.O.; Stippler, E.S. Enzymatic activity in the presence of surfactants commonly used in dissolution media, Part 1: Pepsin. *Results Pharma Sci.* **2016**, *6*, 15–19. [CrossRef] [PubMed]
5. Ly, H.G.T.; Absilis, G.; Janssens, R.; Proost, P.; Parac-Vogt, T.N. Highly amino acid selective hydrolysis of myoglobin at aspartate residues as promoted by Zirconium(IV)-substituted polyoxometalates. *Angew. Chem. Int. Ed.* **2015**, *54*, 7391–7394. [CrossRef] [PubMed]
6. Stroobants, K.; Absillis, G.; Moelants, E.; Proost, P.; Parac-Vogt, T.N. Regioselective hydrolysis of human serum albumin by Zr^{IV}-substituted polyoxotungstates at the interface of positively charged protein surface patches and negatively charged amino acid residues. *Chem. Eur. J.* **2014**, *20*, 3894–3897. [CrossRef]
7. Sap, A.; Absillis, G.; Parac-Vogt, T.N. Selective hydrolysis of oxidized insulin chain B by a Zr(IV)-substituted Wells-Dawson polyoxometalate. *Dalton Trans.* **2015**, *44*, 1539–1548. [CrossRef]
8. Sap, A.; van Tichelen, L.; Mortier, A.; Proost, P.; Parac-Vogt, T.N. Tuning the selectivity and reactivity of metal-substituted polyoxometalates as artificial proteases by varying the nature of the embedded Lewis acid metal ion. *Eur. J. Inorg. Chem.* **2016**, *32*, 5098–5105. [CrossRef]
9. Anyushin, A.V.; Sap, A.; Quanten, T.; Proost, P.; Parac-Vogt, T.N. Selective hydrolysis of Ovalbumin promoted by Hf(IV)-substituted Wells-Dawson-type polyoxometalate. *Front. Chem.* **2018**, *6*, 614. [CrossRef]
10. Stroobants, K.; Moelants, E.; Ly, H.G.T.; Proost, P.; Bartik, K.; Parac-Vogt, T.N. Polyoxometalates as a novel class of artificial proteases: Selective hydrolysis of Lysozyme under physiological pH and temperature promoted by a Cerium(IV) Keggin-type polyoxometalate. *Chem. Eur. J.* **2013**, *19*, 2848–2858. [CrossRef] [PubMed]
11. Ly, H.G.T.; Fu, G.; Kondinski, A.; Bueken, B.; de Vos, D.; Parac-Vogt, T.N. Superactivity of MOF-808 toward peptide bond hydrolysis. *J. Am. Chem. Soc.* **2018**, *140*, 6325–6335. [CrossRef]
12. Moons, J.; de Azambuja, F.; Mihailovic, J.; Kozma, K.; Smiljanic, K.; Amiri, M.; Velickovic, T.C.; Nyman, M.; Parac-Vogt, T.N. Discrete Hf_{18} metal-oxo cluster as a heterogeneous nanozyme for site-specific proteolysis. *Angew. Chem. Int. Ed.* **2020**, *59*, 9094–9101. [CrossRef]
13. Loosen, A.; de Azambuja, F.; Smolders, S.; Moons, J.; Simms, C.; de Vos, D.; Parac-Vogt, T.N. Interplay between structural parameters and reactivity of Zr_6-based MOFs as artificial proteases. *Chem. Sci.* **2020**, *11*, 6662–6669. [CrossRef]
14. Ly, H.G.T.; Fu, G.; de Azambuja, F.; de Vos, D.; Parac-Vogt, T.N. Nanozymatic Activity of UiO-66 metal-organic frameworks: Tuning the nanopore environment enhances hydrolytic activity toward peptide bonds. *ACS Appl. Nano Mater.* **2020**, *3*, 8931–8938. [CrossRef]
15. Nisar, A.; Wang, X. Surfactant-encapsulated polyoxometalate building blocks: Controlled assembly and their catalytic properties. *Dalton Trans.* **2012**, *41*, 9832–9845. [CrossRef]

16. Pope, M.T.; Müller, A. Polyoxometalate chemistry: An old field with new dimensions in several disciplines. *Angew. Chem. Int. Ed.* **1991**, *30*, 34–48. [CrossRef]
17. Proust, A.; Matt, B.; Villanneau, R.; Guillemot, G.; Gouzerh, P.; Izzet, G. Functionalization and post-functionalization: A step towards polyoxometalate-based materials. *Chem. Soc. Rev.* **2012**, *41*, 7605–7622. [CrossRef] [PubMed]
18. Quanten, T.; Shestakova, P.; van Bulck, D.D.; Kirschhock, C.; Parac-Vogt, T.N. Interaction study and reactivity of Zr^{IV}-substituted Wells-Dawson polyoxometalate towards hydrolysis of peptide bonds in surfactant solutions. *Chem. Eur. J.* **2016**, *22*, 3775–3784. [CrossRef] [PubMed]
19. Sap, A.; Vandebroek, L.; Goovaerts, V.; Martens, E.; Proost, P.; Parac-Vogt, T.N. Highly selective and tunable protein hydrolysis by a polyoxometalate complex in surfactant Solutions: A step toward the development of artificial metalloproteases for membrane proteins. *ACS Omega* **2017**, *2*, 2026–2033. [CrossRef]
20. Quanten, T.; de Mayaer, T.; Shestakova, P.; Parac-Vogt, T.N. Selectivity and reactivity of Zr^{IV} and Ce^{IV} substituted Keggin type polyoxometalates toward Cytochrome c in surfactant solutions. *Front. Chem.* **2018**, *6*, 372. [CrossRef] [PubMed]
21. Quanten, T.; Savić, N.D.; Parac-Vogt, T.N. Hydrolysis of peptide bonds in protein micelles promoted by a Zirconium(IV)-substituted polyoxometalate as an artificial protease. *Chem. Eur. J.* **2020**, *26*, 11170–11179. [CrossRef] [PubMed]
22. Tofani, L.; Feis, A.; Snoke, R.E.; Berti, D.; Baglioni, P.; Smulevich, G. Spectroscopic and interfacial properties of myoglobin/surfactant complexes. *Biophys. J.* **2004**, *87*, 1186–1195. [CrossRef] [PubMed]
23. Mondal, S.; Das, S.; Ghosh, S. Interaction of myoglobin with cationic Gemini surfactants in phosphate buffer at pH 7.4. *J. Surfact. Deterg.* **2015**, *18*, 471–476. [CrossRef]
24. Abeyrathne, E.D.N.S.; Lee, H.Y.; Jo, C.; Nam, K.C.; Ahn, D.U. Enzymatic hydrolysis of ovalbumin and the functional properties of the hydrolysates. *Poult. Sci.* **2014**, *93*, 2678–2686. [CrossRef]
25. Huntington, J.A.; Stein, P.E. Structure and Properties of Ovalbumin. *J. Chromatogr. B Biomed. Sci. Appl.* **2001**, *25*, 189–198. [CrossRef]
26. Gettins, P.G.W. Serpin structure, mechanism, and function. *Chem. Rev.* **2002**, *102*, 4751–4804. [CrossRef] [PubMed]
27. Ding, X.; Cai, J.; Guo, X. Effect of surfactant structure on reverse micellar extraction of Ovalbumin. *Process Biochem.* **2015**, *50*, 272–278. [CrossRef]
28. Ting, B.P.C.P.; Pouliot, Y.; Gauthier, S.F.; Mine, Y. Separation, fractionation of egg proteins and peptides for nutraceutical applications. In *Extraction and Concentration Processes in the Food Beverage and Nutraceutical Industries*; Woodhead Publishing: Cambridge, UK, 2013; pp. 595–618.
29. Gasteiger, E.; Gattiker, A.; Hoogland, C.; Ivanyi, I.; Appel, R.D.; Bairoch, A. ExPASy: The proteomics server for in-depth protein knowledge and analysis. *Nucleic Acids Res.* **2003**, *31*, 3784–3788. [CrossRef]
30. Van Rompuy, L.; Savić, N.D.; Rodriguez, A.; Parac-Vogt, T.N. Selective hydrolysis of transferrin promoted by Zr-substituted polyoxometalates. *Molecules* **2020**, *25*, 3472. [CrossRef]
31. Hellmann, N.; Schneider, D. Hands on: Using tryptophan fluorescence spectroscopy to study protein structure. In *Protein Supersecondary Structures*, 2nd ed.; Kister, A.E., Ed.; Springer Science: New York, NY, USA, 2019; pp. 379–401.
32. Favicchio, R.; Dragan, A.I.; Kneale, G.G.; Read, C.M. Fluorescence spectroscopy and anisotropy in the analysis of DNA-protein interactions. In *DNA-Protein Interactions*, 3rd ed.; Leblanc, B., Moss, T., Eds.; Springer: New York, NY, USA, 2009; pp. 589–611.
33. Ly, H.G.T.; Parac-Vogt, T.N. Spectroscopic study of the interaction between horse heart myoglobin and Zirconium(IV)-substituted polyoxometalates as artificial proteases. *Chemphyschem* **2017**, *18*, 2451–2458. [CrossRef]
34. Goovaerts, V.; Stroobants, K.; Absillis, G.; Parac-Vogt, T.N. Molecular interactions between serum albumin proteins and Keggin type polyoxometalates studied using luminescence spectroscopy. *Phys. Chem. Chem. Phys.* **2013**, *15*, 18378–18387. [CrossRef]
35. Stroobants, K.; Goovaerts, V.; Absillis, G.; Bruylants, G.; Moelants, E.; Proost, P.; Parac-Vogt, T.N. Molecular origin of the hydrolytic activity and fixed regioselectivity of a Zr^{IV}-substituted polyoxotungstate as artificial protease. *Chem. Eur. J.* **2014**, *20*, 9567–9577. [CrossRef] [PubMed]
36. Goovaerts, V.; Stroobants, K.; Absillis, G.; Parac-Vogt, T.N. Understanding the regioselective hydrolysis of human serum albumin by Zr(IV)-substituted polyoxotungstates using tryptophan fluorescence spectroscopy. *Inorganics* **2015**, *3*, 230–245. [CrossRef]
37. Vivian, J.T.; Callis, P.R. Mechanisms of tryptophan fluorescence shifts in proteins. *Biophys. J.* **2001**, *80*, 2093–2109. [CrossRef]
38. Vallée-Bélisle, A.; Michnick, S.W. Visualizing transient protein-folding intermediates by tryptophan-scanning mutagenesis. *Nat. Struct. Mol. Biol.* **2012**, *19*, 731–736. [CrossRef]
39. Lakowicz, J.R. *Principles of Fluorescence Spectroscopy*, 3rd ed.; Springer: New York, NY, USA, 2006.
40. Kelly, S.; Price, N. The use of circular dichroism in the investigation of protein structure and function. *Curr. Protein Pept. Sci.* **2000**, *1*, 349–384. [CrossRef]
41. Sreerama, N.; Woody, R.W. Estimation of protein secondary structure from circular dichroism spectra: Comparison of CONTIN, SELCON, and CDSSTR methods with an expanded reference set. *Anal. Biochem.* **2000**, *287*, 252–260. [CrossRef]
42. Whitmore, L.; Wallace, B.A. DICHROWEB, an online server for protein secondary structure analyses from circular dichroism spectroscopic data. *Nucleic Acids Res.* **2004**, *32*, W668–W673. [CrossRef] [PubMed]
43. Whitmore, L.; Wallace, B.A. Protein secondary structure analyses from circular dichroism spectroscopy: Methods and reference databases. *Biopolymers* **2008**, *89*, 392–400. [CrossRef]
44. Zemser, M.; Friedman, M.; Katzhendler, J.; Greene, L.L.; Minsky, A.; Gorinstein, S. Relationship between functional properties and structure of Ovalbumin. *J. Protein Chem.* **1994**, *13*, 261–274. [CrossRef]

45. Dong, A.; Meyer, J.D.; Brown, J.L.; Manning, M.C.; Carpenter, J.F. Comparative fourier transform infrared and circular dichroism spectroscopic analysis of α_1-Proteinase inhibitor and Ovalbumin in aqueous solution. *Arch. Biochem. Biophys.* **2000**, *383*, 148–155. [CrossRef]
46. Bruch, M.; Weiss, V.; Engel, J. Plasma serine proteinase inhibitors (serpins) exhibit major conformational changes and a large increase in conformational stability upon cleavage at their reactive sites. *J. Biol. Chem.* **1988**, *263*, 16626–16630. [CrossRef]
47. González-Pérez, A.; Ruso, J.M.; Prieto, G.; Sarmiento, F. Physicochemical study of Ovalbumin in the presence of sodium dodecyl sulphate in aqueous media. *Colloid Polym. Sci.* **2004**, *282*, 351–356. [CrossRef]
48. Meyer, M.L.; Kauzmann, W. The effects of detergents and urea on the rotatory dispersion of Ovalbumin. *Arch. Biochem. Biophys.* **1962**, *99*, 348–349. [CrossRef]
49. Mattice, W.L.; Riser, J.M.; Clark, D.S. Conformational properties of the complexes formed by proteins and sodium dodecyl sulfate. *Biochemistry* **1976**, *15*, 4264–4272. [CrossRef]
50. Visentini, F.F.; Perez, A.A.; Santiago, L.G. Self-assembled nanoparticles from heat treated ovalbumin as nanocarriers for polyunsaturated fatty acids. *Food Hydrocoll.* **2019**, *93*, 242–252. [CrossRef]
51. Sap, A.; de Zitter, E.; van Meervelt, L.; Parac-Vogt, T.N. Structural characterization of the complex between hen Egg-White Lysozyme and Zr^{IV}-substituted Keggin polyoxometalate as artificial protease. *Chem. Eur. J.* **2015**, *21*, 11692–11695. [CrossRef] [PubMed]
52. Sokolov, M.N.; Chubarova, E.V.; Peresypkina, E.V.; Virovets, A.V.; Fedin, V.P. Complexes of Zr^{IV} and Hf^{IV} with monolacunary Keggin-and Dawson-type anions. *Russ. Chem. Bull.* **2007**, *56*, 220–224. [CrossRef]
53. Wallace, B.A.; Janes, R.W. *Modern Techniques for Circular Dichroism and Synchrotron Radtion Circular Dichroism Spectroscopy*; IOS Press: Amsterdam, The Netherlands, 2009; pp. 1–18.
54. Hunter, R.J. *Foundations of Colloid Science*, 2nd ed.; Oxford Clarendon Press: New York, NY, USA, 2001.